[CANCER RESEARCH 63, 1865–1870, April 15, 2003]

# Overexpression of the *EGFR/FKBP12/HIF-2α* Pathway Identified in Childhood Astrocytomas by Angiogenesis Gene Profiling[1,2]

**Soumen Khatua,[3] Katia M. Peterson,[3] Kevin M. Brown,[3] Christopher Lawlor, Maria R. Santi, Bonnie LaFleur, Devin Dressman, Dietrich A. Stephan, and Tobey J. MacDonald[4]**

*Center for Cancer Research, Children's Research Institute [S. K., K. M. P., C. L., T. J. M.], Research Center for Genetic Medicine, Children's Research Institute [K. M. B., D. D., D. A. S.], and Department of Pathology [M. R. S.], Children's National Medical Center, Washington, DC 20010; Department of Preventative Medicine, Division of Biostatistics, Vanderbilt University, Nashville, Tennessee 37232 [B. L.]; and Graduate Program in Genetics, George Washington University, Washington, DC 20052 [K. M. B.]*

## ABSTRACT

**Intense angiogenesis proliferation, a histopathological hallmark distinguishing malignant from benign astrocytoma, is vital for tumor progression. Thus, identifying and targeting specific pathways that promote malignant astrocytoma-induced angiogenesis could have substantial therapeutic benefit. Expression profiling of 13 childhood astrocytomas to determine the expression pattern of 133 angiogenesis-related genes revealed that 44 (33%) genes were differentially expressed (17 were overexpressed, and 27 were underexpressed) between malignant high-grade astrocytomas (HGAs) and benign low-grade astrocytomas. Hierarchical clustering and principal components analysis using only the 133 angiogenesis-related genes distinguished HGA from low-grade astrocytoma in 100% of the samples analyzed, as did unsupervised analyses using the entire set of 9198 expressed genes represented on the array, indicating that the angiogenesis-related genes were reliable markers of pathological grade. A striking new finding was significant overexpression of *hypoxia-inducible transcription factor (HIF)-2α* as well as high-level expression of *FK506-binding protein (FKBP) 12* by HGA. Furthermore, 9 of 21 (43%) genes overexpressed by HGA were HIF/FKBP-associated genes. This group included the epidermal growth factor receptor (*EGFR*), which promotes HIF synthesis, as well as *insulin-like growth factor-binding protein 2* (*IGFBP2*), a target gene of HIF activity. Differential protein expression of HIF-2α was validated in an independent group of 16 astrocytomas ($P = 0.02$). We conclude that the *EGFR/FKBP12/HIF-2α* pathway is important in childhood HGA and represents a potential new therapeutic target.**

## INTRODUCTION

Astrocytoma is the most common childhood brain tumor, accounting for more than 1000 new cases per year in the United States and 52% of all pediatric brain tumors worldwide (1). Astrocytomas are comprised of a heterogeneous group of glial tumors ranging from the low-grade benign tumors, juvenile pilocytic astrocytoma and diffuse astrocytoma (WHO grade I and II), to the high-grade malignant tumors, anaplastic astrocytoma, and glioblastoma multiforme (WHO grade III and IV). Although chemotherapy can be an effective treatment for LGA,[5] a similar benefit has not been demonstrated in HGA, in which overall survival remains less than 30% (2). Thus, novel therapeutic approaches are needed for childhood HGA.

Studies demonstrating the crucial role of angiogenesis in cancer have been a major advance in our understanding of malignant tumor progression (3). One of the key histopathological features that distinguish HGA from LGA is intense, increased angiogenesis. The invasiveness of HGA, another unique feature of this tumor in comparison with LGA, is associated with increased microvascular density and intratumoral hypoxia (4). Thus, inhibitors of hypoxia-inducible angiogenesis factors could be important new therapeutic agents against HGA. In adults, the most commonly described regulators of brain tumor-derived angiogenesis are VEGF, platelet-derived growth factor, angiopoietin-2, and their respective receptors (5). It is not known to what extent these same regulatory mechanisms exist in pediatric astrocytomas, especially because there are key differences in the common genetic abnormalities observed between adult and childhood astrocytomas that may greatly affect the development of angiogenesis. For instance, although *p53* mutations appear to occur with equal frequency (28–38%) in childhood and adult HGA, the frequency of these mutations in HGA of children younger than 4 years of age is significantly less (6). Furthermore, the incidence of *PTEN* mutations in adult HGA is approximately 30%, whereas the same changes in childhood HGA are rare (7). This is particularly important because studies have shown that wild-type *p53* and *PTEN* expression inhibits angiogenesis induced by malignant astrocytoma cells (8, 9).

In this study we used oligonucleotide microarray profiling (12,626 probe sets) to identify angiogenesis-related genes predictive of childhood HGAs to gain a better understanding of the regulation of malignant angiogenesis in childhood HGA and to identify potential novel therapeutic targets.

## MATERIALS AND METHODS

**Tumor and Cell Line Samples.** Thirteen fresh frozen childhood astrocytoma tissue specimens, including 6 HGAs and 7 LGAs, were obtained from the pediatric division of the Cooperative Human Tissue Network and stored at –80°C until ready for use in the gene expression profiling studies. Two HGA cell lines, U-87 MG and CCF-STTG1, were obtained from the American Type Culture Collection and grown according to American Type Culture Collection recommendations. All of the tissue specimens and cell lines were used for gene expression profiling. Seventeen additional paraffin-embedded tissue specimens, including 8 HGAs, 8 LGAs, and 1 normal control cortical brain, were obtained from the pathology department of Children's National Medical Center and used for protein confirmation of selected gene products by immunohistochemistry. The Children's National Medical Center Institutional Review Board approved all studies performed.

**Gene Expression Profiling.** Total RNA was isolated from the tissues and cell lines using TRIzol reagent as described previously (10). Briefly, a minimum of 10–25 μg of total RNA was obtained from each tumor tissue sample and cell line. Ten μg of extracted RNA from each sample were synthesized into double-stranded cDNA with the SuperScript choice system (Life Technologies, Inc., Carlsbad, CA) using an oligo(dT) primer containing a T7 RNA polymerase promoter (Genset, San Diego, CA). The double-stranded cDNA was purified by phenol-chloroform extraction and *in vitro* transcribed using the ENZO Bioarray RNA transcript labeling kit (Affymetrix, Santa Clara, CA).

Received 9/12/02; accepted 2/14/03.

The costs of publication of this article were defrayed in part by the payment of page charges. This article must therefore be hereby marked *advertisement* in accordance with 18 U.S.C. Section 1734 solely to indicate this fact.

[1] Supported by NIH Grant K08 CA92056-01A1, an Avery Research Scholarship from Children's Research Institute, and the Childhood Brain Tumor Foundation [T. J. M. and K. M. P.] and by National Institute of Neurological Disorders and Stroke Grant 1U24NS43571-01 [to D. A. S. and K. M. B.].

[2] Supplementary data for this article are available at Cancer Research Online (http://cancerres.aacrjournals.org).

[3] These authors contributed equally to this work.

[4] To whom requests for reprints should be addressed, at Department of Hematology/Oncology, Center for Cancer Research, Children's National Medical Center, 111 Michigan Avenue NW, Washington, DC 20010. Phone: (202) 884-2146; Fax: (202) 884-5685; E-mail: tmacdona@cnmc.org.

[5] The abbreviations used are: LGA, low-grade astrocytoma; HGA, high-grade astrocytoma; VEGF, vascular endothelial growth factor; HIF, hypoxia-inducible factor; PCA, principal components analysis; FKBP, FK506-binding protein; EGFR, epidermal growth factor receptor; FRAP, FK506-binding protein rapamycin-associated protein; PGK1, phosphoglycerate kinase 1; RT-PCR, reverse transcription-PCR.

The biotin-labeled cRNA was purified using the RNeasy kit (Qiagen, Valencia, CA) and then fragmented to approximately 200 bp by alkaline treatment [200 mM Tris-acetate (pH 8.2), 500 mM potassium acetate, and 150 mM magnesium acetate]. Each cRNA was hybridized to an Affymetrix U95Av2 array containing approximately 12,000 human transcripts and detected using a streptavidin-conjugated fluor and confocal laser scanning according to the manufacturer's recommendations (Affymetrix). Data were extracted using Microarray Suite Version 4.0 (Affymetrix) and linearly scaled such that the average intensity across each chip equaled 800. Data from a chip were rejected if the ratio of the average intensity of the 3′ to 5′ ends of the human glyceraldehyde-3-phosphate dehydrogenase gene exceeded 3, or if the linear scaling factor exceeded 4. Genes not called "present" for any of the samples, as determined by the Affymetrix software, were excluded from further consideration. To avoid division by zero or negative numbers in the calculation of average fold differences between sample classes, values of 10 or less were set to 10. Subsequent statistical methods used the complete data set in which values less than 10 were not adjusted. All raw expression values can be downloaded from online supplementary data.[2] Gene ontology annotations for genes represented on the U95Av2 chip were compiled from the Affymetrix NetAffx analysis website.[6]

**RT-PCR Analysis.** PCR amplification was performed directly on the T7-dT primered double-stranded cDNA (originally generated for expression profiling) from three LGAs and three HGAs. Each cDNA was diluted 100-fold, and 5 $\mu$l of the diluted cDNA were used as template for each PCR. $\beta$-Actin was used as internal control. Gene-specific primers from Invitrogen Life Technologies, Inc. [EGFR, 5′-tgcagcgatacagctcagaccc-3′ (forward primer) and 5′-tttgggaacggactggtttatg-3′ (reverse primer); IGFBP2, 5′-tgacaagcatggcctgtacaac-3′ (forward primer) and 5′-ggatcagcttcccggtgttg-3′ (reverse primer); HIF-2$\alpha$, 5′-agcctccatctgccatcagtc-3′ (forward primer) and 5′-cttgccatgcctgacaccttg-3′ (reverse primer); and $\beta$-actin, 5′-acgtgtacgccaacacagtg-3′ (forward primer), 5′-gccatgccaatctcatctt-3′ (reverse primer)] were used in a 50-$\mu$l reaction consisting of 1× PCR Gold Buffer, 2.25 mM $MgCl_2$, 0.2 mM deoxynucleoside triphosphates, 2 units of TaqGold polymerase, and 12 pmol of each primer. Initial denaturation (94°C, 12 min) was followed by 30 cycles of denaturation (94°C, 30 s), annealing (57°C, 30 s), and extension (72°C, 45 s). This was followed by a final extension step (72°C, 5 min). Four $\mu$l of $\beta$-actin product were combined with 8 $\mu$l of EGFR, IGFBP2, or HIF-2$\alpha$ product for each sample; electrophoresed on a 1.5% agarose gel stained with ethidium bromide; and visualized with UV light. Product bands were quantitated by volume densitometry using Quantity One software (Bio-Rad, Hercules, CA), and signals were normalized to actin.

**Selection of Genes Involved in Angiogenesis.** The expression profile of 133 angiogenesis-related genes was specifically selected for analysis from the 9,198 total probe sets with detectable expression in the astrocytoma samples of the 12,626 total probe sets analyzed on the array. For genes represented on the array with more than one probe set, the probe set that was called "present" in the greatest number of samples by the Microarray Suite Version 4.0 software was chosen as the "best" representative for that gene. If the number of present calls was equal for more than one probe set, then the probe set with the highest average numerical expression value across all of the samples was chosen as the "best" representative. Designation of known genes associated with angiogenesis was based on extensive review of available published literature databases.

**Hierarchical Clustering and PCA.** As a means to examine data structure, hierarchical clustering and PCA were performed on the complete microarray dataset (9,198 probe sets called present in at least one sample) as well as on the limited dataset of 133 preselected angiogenesis-specific genes. Hierarchical clustering dendrograms, as well as the graphical representation of the data for the statistically significant angiogenesis-related genes, were generated using downloaded Cluster and TreeView software[7] (written by Michael Eisen). All clustering was performed using the uncentered-correlation and complete linkage clustering options. Data represented in clustergrams are normalized intensities. Two-dimensional PCA plots were generated using the PCA scores of the two components accounting for the greatest intersample variability as calculated by the Cleaver 1.0 website (Stanford University).[8]

[6] http://www.affymetrix.com.
[7] http://rana.lbl.gov.
[8] http://classify.stanford.edu/.

**Statistical Methods and Selection of Differentially Expressed Genes.** We used permutational *P*s less than or equal to 0.05 to select our candidate gene list. Our permutation tests were performed to determine which genes showed significant differences in mean intensity between the classes. To determine a permutational *P* for each gene, we first calculated the mean and variances for the sample intensities within each class and calculated a *t* test statistic ($\hat{\theta}$). The class assignments of the tumors were subsequently permuted, using sampling without replacement, 50,000 times. For each permutation we calculated a test statistic $\theta^*_{(i)}$ for all $i = 1, \ldots, 50{,}000$ permutations. The permutational *P* is the probability of observing at least as large a value for the test statistic for any random permutation [$\theta^*_{(i)}$] as for our initial test statistic ($\hat{\theta}$). This method has the benefit of not depending on distributional assumptions.

**Protein Validation by Immunohistochemistry.** Sixteen formalin-fixed paraffin-embedded astrocytoma tissues (8 HGAs and 8 LGAs) as well as one normal control cortical brain were cut into 4-$\mu$m-thick sections. Standard immunohistochemistry was performed as described previously in detail (10). Antibodies for HIF-1$\alpha$ were obtained from US Biologicals (Swampscott, MA), and antibodies for HIF-2$\alpha$ were obtained from Novus Biologicals (Littleton, CO). Three authors independently reviewed the slides and graded the staining as absent (−), weak (+), moderate (++), and strong (+++). The staining was then correlated with the grades of tumors (WHO I−IV) and with RNA expression levels obtained by the microarray experiments. Significance of differential protein expression was evaluated by comparing the number of HGA and LGA specimens with positive (+, ++, and +++) and negative (−) staining using the one-tailed Fischer's exact test.

## RESULTS

**Expression Profiling of Astrocytomas.** The expression profile of 12,626 probe sets was obtained in 13 individual pediatric astrocytomas and 2 HGA cell lines. A total of 133 genes that are known or have been reported to be associated with angiogenesis were specifically compared between the expression profiles generated by the HGA and LGA samples in a supervised fashion. Of the 133 angiogenesis-related genes that were chosen *a priori*, 44 (33%) were differentially expressed ($P < 0.05$; Fig. 1*A*). Of the 44 differentially expressed genes, 17 were up-regulated in HGA, and 27 were down-regulated in HGA. Several of these genes were noted to be related to the regulation of the HIF pathway. Thus, we further selected 11 genes on the array that were also related to HIF but had not previously been described as being directly associated with angiogenesis. Subsequent analysis of 11 HIF-related genes showed that nearly half were differentially expressed. A summary of the expression data for both the 133 preselected angiogenesis genes and the 11 HIF-related genes is included in the online supplementary data. RT-PCR analysis for three key genes, *EGFR*, *IGFBP2*, and *HIF-2α*, independently confirmed the microarray expression results (Fig. 2).

**Classification of Tumor Samples.** To visualize the underlying structure of gene expression in the dataset, we performed unsupervised hierarchical clustering on all 9198 probe sets with detectable expression in any of the astrocytomas (Fig. 1*B*). The HGA and LGA specimens clustered onto separate branches of the sample dendrogram, suggesting that the patterns of gene expression are more alike within a tumor class than between tumor classes. We also performed PCA, another method that may be used to visualize the underlying structure of gene expression data, on the complete set of 9198 expressed probes (11). PCA is a data reduction method that takes into account all measurements in the dataset and defines a smaller set of linearly combined measurements (or components) that retain the maximum amount of information present in the original data. Like the hierarchical clustering results, a plot of the two principal components that explain the most intersample variation suggests that there is underlying structure to the data that distinguishes the two classes of astrocytomas (Fig. 1*D*). The low-grade tissue samples are clearly

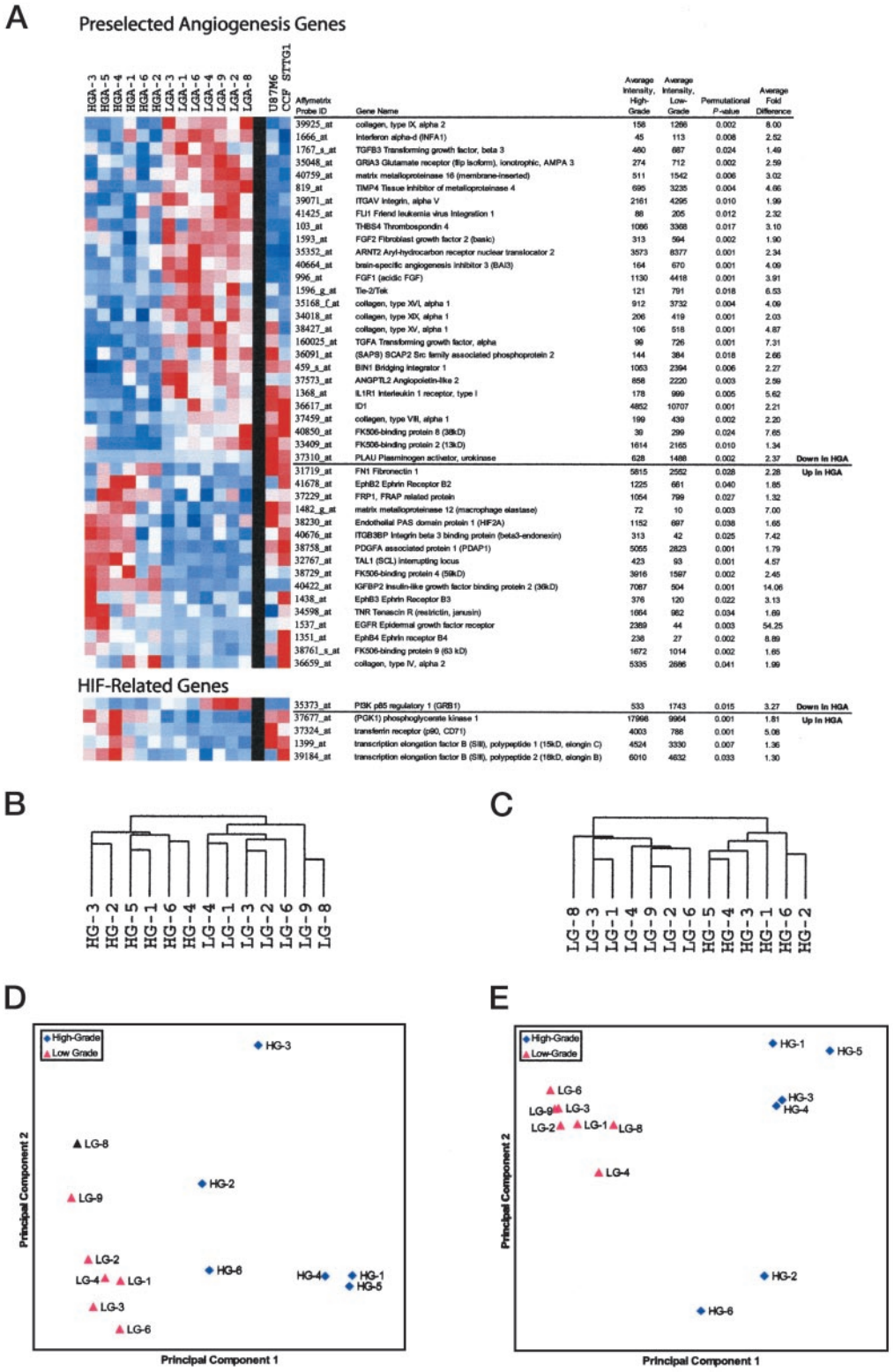


Fig. 1. *A*, expression profile of statistically significant angiogenesis-related genes, as well as HIF-related genes, that are differentially expressed in HGAs *versus* LGAs. Levels of expression are represented on a scale from *red* (lowest expression) to *blue* (highest expression). *B*, sample dendrogram generated using unsupervised hierarchical clustering on all 9198 probe sets expressed in astrocytomas. HGA and LGA samples cluster onto separate dendrogram branches. *C*, hierarchical clustering using only 133 angiogenesis-specific genes chosen *a priori* also separates HGA from LGA. *D*, two-dimensional PCA plot generated from unsupervised PCA using all 9198 expressed probe sets. HGA and LGA specimens are separated based on the single component accounting for the most variability in the data (principal component 1). *E*, PCA using only angiogenesis-specific genes also shows separation of HGA from LGA samples based on principal component 1.

A

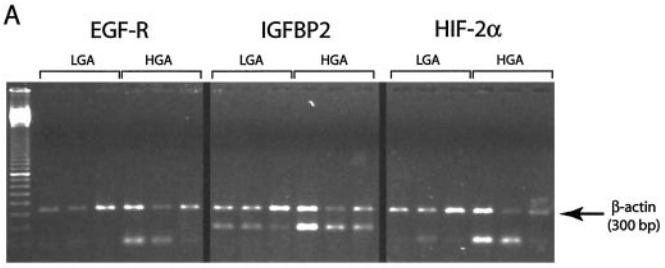


B

| Gene Identity | Sample Grade | Band Density: Validation Gene | Band Density: β-Actin Control | Ratio (Gene/Actin) |
|---|---|---|---|---|
| EGF-R | LGA | 636 | 855 | 0.74 |
| | LGA | 728 | 817 | 0.89 |
| | LGA | 724 | 1449 | 0.50 |
| | HGA | 1425 | 1542 | 0.92 |
| | HGA | 1147 | 942 | 1.22 |
| | HGA | 889 | 1307 | 0.68 |
| IGFBP2 | LGA | 1208 | 1383 | 0.87 |
| | LGA | 1177 | 1378 | 0.85 |
| | LGA | 1016 | 1787 | 0.57 |
| | HGA | 2130 | 1862 | 1.14 |
| | HGA | 1494 | 1102 | 1.36 |
| | HGA | 1390 | 1416 | 0.98 |
| HIF-2α | LGA | 903 | 1428 | 0.63 |
| | LGA | 1055 | 1325 | 0.80 |
| | LGA | 893 | 1731 | 0.52 |
| | HGA | 1888 | 1750 | 1.08 |
| | HGA | 1590 | 922 | 1.72 |
| | HGA | 692 | 959 | 0.72 |

Fig. 2. Confirmation of array data by RT-PCR analysis. *A*, agarose gel electrophoresis analysis of RT-PCR products obtained from LGAs and HGAs using the gene-specific primers for EGF-R, HIF-2$\alpha$, and IGFBP2, using $\beta$-actin as an internal control. *B*, signals for each tumor were normalized to that of the $\beta$-actin internal control.

separated from the high-grade samples by principal component 1 (explains 21.1% of the variability), indicating that tumors within a sample class contain similar gene expression information.

To explore the possibility that such a structure may exist in the smaller subset of 133 genes chosen for a role in angiogenesis, we performed hierarchical clustering and PCA on this subset of data (Fig. 1, *C* and *E*). As with the larger dataset, the two tumor classes clustered into separate dendrogram branches. PCA also distinguished the tumor classes using only a single component (principal component 1, explaining 24.2% of the variability). The most frequently occurring ontologies in the categories of biological process, cell component, and molecular function are summarized in the online supplementary data.

**Immunohistochemical Staining for HIF Proteins.** We performed immunohistochemical protein validation for HIF-1$\alpha$ and HIF-2$\alpha$ in an independent set of 16 tumor tissues (8 HGAs and 8 LGAs) as well as a section of normal cortical brain. Representative images are shown in Fig. 3. Absent to minimal staining was observed for HIF-1$\alpha$ in normal brain (Fig. 3*A*) as well as in LGA (Fig. 3*B*) and HGA (Fig. 3*C*). Although there is some background staining, there is no definite cellular staining. In contrast, positive staining was observed for HIF-2$\alpha$ in astrocytoma specimens. Staining was observed primarily in HGA specimens (Fig. 3, *F* and *G*), often around the leading invasive tumor edges. Comparison of the number of positively (+, ++, and +++ combined) and negatively (−) staining slides for HIF-2$\alpha$ showed significant overexpression of HIF-2$\alpha$ protein in HGA in comparison with LGA ($P = 0.02$), as shown in Fig. 3*H*.

## DISCUSSION

Expression of HIFs and the target genes that promote angiogenesis is critical for the growth and invasiveness of astrocytomas. Pathology of malignant HGA is distinguished from LGA by intense proliferation of angiogenesis. Thus, inhibiting angiogenesis should have therapeutic benefit, particularly in childhood HGA, in which chemotherapy has not been effective. We addressed this question by comparing pediatric HGA and LGA using microarray profiling and focused analysis of angiogenesis genes.

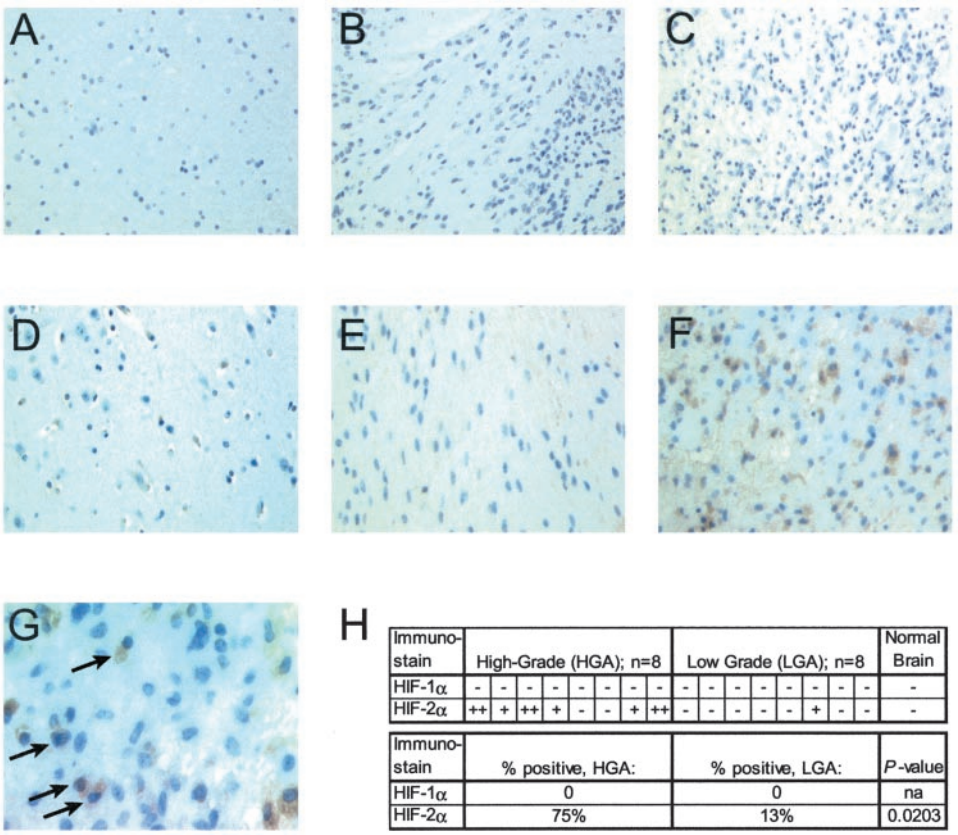


H

| Immunostain | High-Grade (HGA); n=8 | | | | | | | | Low Grade (LGA); n=8 | | | | | | | | Normal Brain |
|---|---|---|---|---|---|---|---|---|---|---|---|---|---|---|---|---|---|
| HIF-1α | - | - | - | - | - | - | - | - | - | - | - | - | - | - | - | - | - |
| HIF-2α | ++ | + | ++ | + | - | - | + | ++ | - | - | - | - | - | + | - | - | - |

| Immunostain | % positive, HGA: | % positive, LGA: | *P*-value |
|---|---|---|---|
| HIF-1α | 0 | 0 | na |
| HIF-2α | 75% | 13% | 0.0203 |

Fig. 3. Immunohistochemical protein validation of HIF-1$\alpha$ and HIF-2$\alpha$ on normal brain, and an independent set of LGA and HGA. Normal brain (*A*), LGA (*B*), and HGA (*C*) showed no significant staining for HIF-1$\alpha$. Staining of normal brain (*D*), LGA (*E*), and HGA (*F*) against HIF-2$\alpha$ is shown. All sections photographed at ×200. *G*, ×400 magnification of HGA stained against HIF-2$\alpha$. *Arrows* indicate malignant cells positively stained for HIF-2$\alpha$. *H*, summary of tissue staining for HIF-1$\alpha$ and HIF-2$\alpha$. Tissue sections were scored for absent (−), weak (+), moderate (++), or strong (+++) staining. Significance of differential HIF-2$\alpha$ protein expression was evaluated by comparing the number of samples with positive (+, ++, +++) and negative (−) staining using the one-tailed Fischer's exact test.

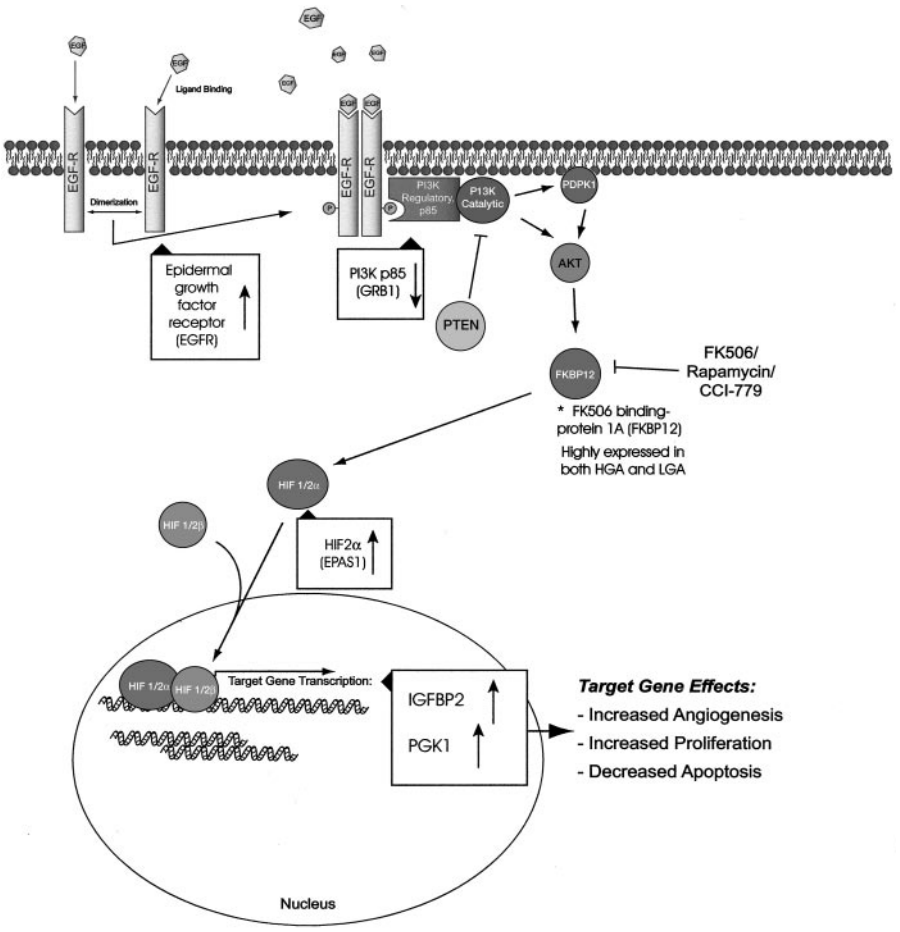


Fig. 4. Schema showing pathway of EGFR/FKBP12/HIF-2$\alpha$ activation. *Boxes* denote genes differentially expressed at the mRNA level between HGA and LGA. Genes with *up arrows* are overexpressed in HGA relative to LGA; genes with *down arrows* are underexpressed in HGA relative to LGA.

On the microarray, 9198 genes had above-threshold expression in at least one astrocytoma. Of these genes, 2401 (26%) were differentially expressed between HGA and LGA with a permutational $P < 0.05$. Thus, there is a marked difference in the expression patterns of the HGA and LGA specimens tested, and the largest proportion of differential genes is involved in signal transduction and gene transcription.

Using all probe sets (9198) expressed in the tumor samples, high- and low-grade tumors separated into different dendrogram branches by hierarchical clustering. Additionally, PCA using this same gene set yielded separation of the samples using only the one component explaining the largest proportion of variability in the dataset. The separation of the tumor classes using such unsupervised methods is not surprising, given the differences in expression of a large proportion of genes between malignant and benign astrocytomas. More striking were the considerable differences in the expression of the 133 angiogenesis-related genes that were chosen for examination *a priori*. Using only this gene list, hierarchical clustering and PCA separated the tumor classes into two distinct groups in a manner similar to that observed in the unsupervised methods using all genes. This indicates that the angiogenesis gene expression profile alone is an accurate predictor of pathological grade in astrocytoma. Not surprisingly, a large proportion of the angiogenesis-related genes (36%) showed marked expression differences between sample classes.

By focusing analysis on angiogenesis genes, we identified overexpression of *HIF-2α* in HGA for the first time in childhood astrocytoma. *HIF-2α* encodes a basic helix-loop-helix PAS domain protein transcription factor that regulates vascular maturation, remodeling, and stabilization of angiogenesis in response to hypoxia (12). Unlike the related transcription factor *HIF-1α*, which was found to be similarly expressed in HGA and LGA, *HIF-2α* was differentially overexpressed by HGA at the mRNA level ($P = 0.003$). This differential expression was confirmed to be significant at the protein level as well ($P = 0.02$). Expression of HIF-1$\alpha$ has been shown in adult HGA and oligodendroglioma (13). HIF-2$\alpha$ is strongly expressed in breast carcinoma and is associated with high vascular grade and poor survival (14).

The synthesis of HIF-2$\alpha$ is induced via a signal transduction pathway initiated by receptor tyrosine kinases, such as the EGFR. This leads to activation of phosphatidylinositol 3′-kinase, protein kinase B (AKT), and FRAP, also known as mammalian target for rapamycin (15). We show that *EGFR* mRNA is differentially up-regulated in HGA ($P = 0.003$). This is a consistent finding in adult HGA (16). Furthermore, we found multiple FKBPs, especially *FKBP12*, to be highly expressed in LGA, HGA, and astrocytoma cells. More importantly, the largest group of functionally related, differentially overexpressed genes is comprised of members of the *EGFR/FKBP12/HIF-2α* pathway, constituting nearly one-fourth of all of the up-regulated angiogenesis genes in HGA. Interestingly, the phosphatidylinositol 3′-kinase regulatory unit upstream of FKBP12, *p85*, is down-regulated in HGA, suggesting dysregulation of this pathway via EGFR overexpression. These data implicate the *EGFR/FKBP12/HIF-2α* pathway as an important promoter of angiogenesis in childhood HGA.

Expression of HIF-2$\alpha$ results in the induction of several target genes such as *Glut-1*, *VEGF*, and *PGK1* (17). These genes are responsible for angiogenic and metabolic changes resulting in increased microvascular density and tumor growth. *Glut-1* was not differentially expressed in the astrocytomas analyzed. However, *PGK1* was highly expressed in HGA, LGA, and both cell lines and

was differentially overexpressed in HGA ($P = 0.01$). PGK1 is secreted by tumor cells and reduces disulfide bonds in the serine proteinase plasmin to release the microvessel inhibitor angiostatin (18). Although *VEGF* was highly expressed in HGA, LGA, and astrocytoma cells, it was not differentially expressed. This is in contrast to that seen in adults (19). These data suggest that HIF-induced expression of *PGK1*, previously undescribed in astrocytoma, may be critical to the promotion of the malignant angiogenic phenotype in childhood HGA.

Other genes typically associated with angiogenesis in adult HGA, such as *platelet-derived growth factor*, *angiopoietin-2*, and their receptors, were also highly expressed yet not significantly different in expression levels between LGA and HGA. Interestingly, our study shows that 24% of all of the preselected angiogenesis-related genes that were differentially expressed between HGA and LGA belonged to the families of extracellular matrix and proteases such as collagen, matrix metalloproteinases, and urokinase.

Fig. 4 diagrams the pathway of EGFR/FKBP12/HIF-2$\alpha$ activation and highlights the large proportion of genes in this pathway that were found to be overexpressed by HGA in our study. Taken together, these findings could have direct therapeutic importance. For example, FK506 and rapamycin are structurally related immunosuppressants that block distinct stages in intracellular signaling pathways by binding to members of the FRAP/FKBP12 immunophilin family and down-regulating signals through S6 kinase and FRAP, affecting the expression level of mRNA important for progression from $G_1$ to S phase (20). Because hypoxia enhances angiogenesis through FRAP/FKBP12 signaling, blocking this pathway may have potent antineoplastic effects. Thus, our findings raise the distinct possibility that rapamycin analogues and HIF-2 inhibitors could be useful as therapeutic agents in pediatric HGA.

## REFERENCES


1. Gurney, J. G. Topical topics: brain cancer incidence in children: time to look beyond the trends. Med. Pediatr. Oncol., *33*: 110–112, 1999.
2. Cohen, K. J., Broniscer, A., and Glod, J. Pediatric glial tumors. Curr. Treat. Options Oncol., *2:* 529–536, 2001.
3. Hockel, M., and Vaupel, P. Tumor hypoxia: definitions and current clinical, biologic and molecular aspects. J. Natl. Cancer Inst. (Bethesda), *93:* 266–276, 2001.
4. Semenza, G. L. Hypoxia-inducible factor 1: oxygen homeostasis and disease pathophysiology. Trends Mol. Med., *7:* 345–350, 2001.
5. Ding, H., Roncari, L., Wu, X., Lau, N., Shannon, P., Nagy, A., and Guha, A. Expression and hypoxic regulation of angiopoietins in human astrocytomas. Neuro-oncol., *3:* 1–10, 2001.
6. Pollack, I. F., Finkelstein, S. D., Burnham, J., Holmes, E. J., Hamilton, R. L., Yates, A. J., Finlay, J. L., and Sposto, R. Age and TP53 mutation frequency in childhood malignant gliomas: results in a multi-institutional cohort. Children's Cancer Group. Cancer Res., *61:* 7404–7407, 2001.
7. Raffel, C., Frederick, L., O'Fallon, J. R., Atherton-Skaff, P., Perry, A., Jenkins, R. B., and James, C. D. Analysis of oncogene and tumor suppressor gene alterations in pediatric malignant astrocytomas reveals reduced survival for patients with PTEN mutations. Clin. Cancer Res., *5:* 4085–4090, 1999.
8. Van Meir, E. G., Polverini, P. J., Chazin, V. R., Su Huang, H. J., de Tribolet, N., and Cavenee, W. K. Release of an inhibitor of angiogenesis upon induction of wild type p53 expression in glioblastoma cells. Nat. Genet., *8:* 171–176, 1994.
9. Wen, S., Stolarov, J., Myers, M. P., Su, J. D., Wigler, M. H., Tonks, N. K., and Durden, D. L. PTEN controls tumor-induced angiogenesis. Proc. Natl. Acad. Sci. USA, *98:* 4622–4627, 2001.
10. MacDonald, T. J., Brown, K. M., LaFleur, B., Peterson, K. M., Lawlor, C., Chen, Y., Packer, R. J., Cogen, P., and Stephan, D. A. Expression profiling of medulloblastoma: PDGFRA and the RAS/MAPK pathway as therapeutic targets for metastatic disease. Nat. Genet., *29:* 143–152, 2001.
11. Misra, J., Schmitt, W., Hwang, D., Hsiao, L. L., Gulans, S., and Stephanpoulas, G. Interactive exploration of microarray gene expression patterns in a reduced dimensional space. Genome Res., *12:* 1112–1120, 2002.
12. Weisener, S. M., Turley, H., Allen, E. W., Williams, C., Eckardt, K. U., Talks, L. K., Wood, M. S., Gatter, C. K., Harris, L. A., Pugh, W. C., Ratcliffe, J. P., and Maxwell, H. P. Induction of endothelial PAS domain protein-1 by hypoxia: characterization and comparison with hypoxia-inducible factor-1. Blood, *92:* 2260–2268, 1998.
13. Zagzag, D., Zhong, H., Scalzitti, J. M., Laughner, E., Simons, J. W., and Semenza, G. L. Expression of hypoxia-inducible factor 1$\alpha$ in brain tumors: association with angiogenesis, invasion and progression. Cancer (Phila.), *88:* 2606–2618, 2000.
14. Leek, R. D., Talks, K. L., Pezzella, F., Turley, H., Campo, L., Brown, N. S., Bicknell, R., Taylor, M., Gatter, K. C., and Harris, A. L. Relation of hypoxia-inducible factor-2$\alpha$ (HIF-2$\alpha$) expression in tumor-infiltrative macrophages to tumor angiogenesis and the oxidative thymidine phosphorylase pathway in human breast cancer. Cancer Res., *62:* 1326–1329, 2002.
15. Muthuswamy, S. K., Gilman, M., and Brugge, J. S. Controlled dimerization of ErbB receptors provides evidence for differential signalling by homo-and heterodimers. Mol. Cell. Biol., *19:* 6845–6857, 1999.
16. Liu, W., James, C. D., Frederick, L., Alderete, B. E., and Jenkins, R. B. PTEN/MMAC1 mutations and EGFR amplification in glioblastomas. Cancer Res., *57:* 5254–5257, 2002.
17. Seagroves, T., and Johnson, R. S. Two HIFs may be better than one. Cancer Cell, *1:* 211–213, 2002.
18. Lay, A. J., Jiang, X. M., Daley, E., Sun, L., and Hogg, P. J. Plasmin reduction by phosphoglycerate kinase is a thiol-independent process. J. Biol. Chem., *277:* 9026–9028, 2002.
19. Chan, A. S., Leung, S. Y., Wong, M. P., Yuen, S. T., Cheung, N., Fan, Y. W., and Chung, L. P. Expression of vascular endothelial growth factor and its receptors in the anaplastic progression of astrocytoma, oligodendroglioma, and ependymoma. Am. J. Surg. Pathol., *22:* 816–826, 1998.
20. Hidalgo, M., and Rowinsky, E. K. The rapamycin-sensitive signal transduction pathway as a target for cancer therapy. Oncogene, *19:* 6680–6686, 2000.

# Overexpression of the *EGFR/FKBP12/HIF-2α* Pathway Identified in Childhood Astrocytomas by Angiogenesis Gene Profiling

Soumen Khatua, Katia M. Peterson, Kevin M. Brown, et al.

*Cancer Res* 2003;63:1865-1870.